



Optimization of a supersonic transport aircraft propulsion system

Downloaded from: <https://research.chalmers.se>, 2026-04-19 05:02 UTC

Citation for the original published paper (version of record):

Habibniarami, M., Lundbladh, A., Rizzi, A. et al (2026). Optimization of a supersonic transport aircraft propulsion system. *Aerospace Science and Technology*, 175.

<http://dx.doi.org/10.1016/j.ast.2026.111943>

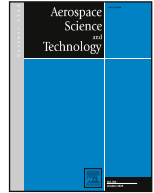
N.B. When citing this work, cite the original published paper.



ELSEVIER

Contents lists available at ScienceDirect

Aerospace Science and Technology

journal homepage: www.elsevier.com/locate/aescte

Original article

Optimization of a supersonic transport aircraft propulsion system

Mehdi Habibniarami ^{a,*}, Anders Lundbladh ^b, Arthur Rizzi ^c, Jesper Ooppelstrup ^c,
Tomas Grönstedt ^a^a Chalmers University of Technology, Gothenburg, SE-412 96, Sweden^b Dept, GKN Aerospace, Trollhättan, 9637 - TL3S SE-461 81, Sweden^c Royal Institute of Technology (KTH), Stockholm, 100 44, Sweden

ARTICLE INFO

Communicated by Kontis Konstantinos

Keywords:

Supersonic transport aircraft
Aerothermodynamics
Propulsion efficiency
Optimization analysis
Design and off-design performance

ABSTRACT

An aerothermodynamic performance analysis is conducted for a supersonic transport propulsion system, evaluating the feasibility of a single-stage and a two-stage fan configuration. The propulsion system is modeled using a parametric approach, incorporating variations in fan pressure ratio, bypass ratio, and high-pressure turbine inlet temperature to assess their impact on cruise and off-design performance. A two-shock external compression intake is assumed. The analysis is performed for a cruise speed of Mach 1.7 at an altitude of 60,000 feet, similar to the cruise conditions proposed for the Boom aircraft. The results demonstrate that the two-stage fan configuration offers superior performance, achieving an 8.5% increase in specific range compared to the single-stage fan while maintaining a reduced fan diameter and lower overall engine mass. The off-design analysis reveals a significant performance penalty associated with the long-proposed idea of boom-less, overland supersonic cruise. A 22% reduction in specific range is predicted when shifting from a Mach 0.95 to Mach 1.2 over land cruise. The off-design analysis further highlights the efficiency advantages of the two-stage fan, with a 3.5% reduction in specific fuel consumption at lower Mach numbers and a broader operational envelope.

1. Introduction

Civil supersonic transport (SST) has been pursued at least since the mid 1950s [1,2]. Development focusing on the high-speed aviation transport, especially for the intercontinental flights has been launched by the National Aeronautics and Space Administration (NASA), aerospace industries, and universities over 60 years ago [3,4]. Early US development focused on a swing-wing concept, the Boeing 2707, targeting very high cruise speeds of around 2.7 Mach [5]. Soviet and European efforts have followed similar routes culminating with the British/French Mach 2+ design, the Concorde, becoming an iconic product claiming the early SST achievements [6]. It stayed in service for over 25 years until the International Civil Aviation Organization (ICAO) announced the termination of the SST fleet in 2003, primarily based on environmental concerns but also due to the difficulties maintaining commercial profitability [7,8]. Compared to the subsonic flights, its fuel consumption per passenger per distance traveled, its atmospheric pollution, and the sonic boom gradually rendered it infeasible [9].

After more than two decades without SST flights, there has been a renewed interest in reviving the concept to a potentially operational status. According to the reports [10–12] on SST market analysis, it was

anticipated that we should already have had some hundred units of supersonic jets available by now. Roy Harris [6], a chief director of aeronautics and high-speed flights at NASA, indicated that by early 2000 we will be on the threshold of having a viable supersonic commercial fleet for long-range destinations. Based on the advancements in technology, Sun and Smith [13] heightened the expectations of low-boom low-drag designs capable of meeting stringent regulatory requirements. The supersonic airliner Boom Overture [14] is targeting a 65–80 passenger Mach 1.7 aircraft to be fully ready for flight by 2025. They have reported successful flight tests with their 1/3 scale test aircraft, the XB-1 [15].

Through NASA's efforts new SST concepts have gradually evolved within the Supersonic Technology Concept Aeroplanes (STCAs) studies and more recently by intensifying research in low-boom designs which led to the launch of the CST program on commercial supersonic technology, aiming to find low noise supersonic overland capability [16]. For the 2025–2035 time frame (N+3), the development of a 100+ passenger aircraft with acceptable acoustic performance and fuel efficiency goals is deemed feasible [17].

Since there has not been a regulated standard for the environmental aspects of SSTs, ICAO launched a program with NASA to establish clear

* Corresponding author.

E-mail addresses: mehdi.habibniarami@chalmers.se (M. Habibniarami), anders.lundbladh@gknaerospace.com (A. Lundbladh), rizzi@kth.se (A. Rizzi), jespero@kth.se (J. Ooppelstrup), tomas.gronstedt@chalmers.se (T. Grönstedt).<https://doi.org/10.1016/j.ast.2026.111943>

Received 9 January 2026; Received in revised form 12 February 2026; Accepted 15 February 2026

Available online 20 February 2026

1270-9638/© 2026 The Author(s). Published by Elsevier Masson SAS. This is an open access article under the CC BY license (<http://creativecommons.org/licenses/by/4.0/>).

Nomenclature*Roman Symbols*

b	Wingspan (m)
C_D	Drag coefficient
C_{D0}	Zero-lift drag coefficient
C_k	Wing chord length at kink (m)
C_L	Lift coefficient
C_r	Wing chord length at root (m)
C_t	Wing chord length at tip (m)
D	Drag (N)
F	Thrust (N)
FPR, π_{fan}	Fan pressure ratio
L	Lift force (N)
L/D	Lift-to-drag ratio
L_f	Aircraft length (m)
M	Mach number
M_{mid}	Mid-cruise aircraft mass
\dot{m}	Intake mass flow rate (kg/s)
\dot{m}_a	Core air mass flow rate (kg/s)
\dot{m}_c	Cooling-air mass flow rate (kg/s)
OPR	Overall pressure ratio
P	Pressure (Pa)
Re	Reynolds number
SFC	Specific fuel consumption (mg/N-s)
SR	Specific range (m/kg)
S_{ref}	Reference Area (m ²)
S_w	Wetted Area (m ²)
T	Static temperature (K)
T_3	Compressor exit temperature (K)
T_4	Turbine inlet temperature (K)
V	True airspeed (m/s)
W	Aircraft weight (N)
Y_k	kink span (m)
Y_t	Tip span (m)

Subscripts and Superscripts

0	Freestream (ambient)
1	Intake entry
1st	single-stage fan
2st	two-stage fan
3	High-pressure compressor output

4	High-pressure turbine inlet
5	Low-pressure turbine exit
5'	Bypass duct exit
des	design
HPC	High-pressure compressor
HPT	High-pressure turbine
ISA	International Standard Atmosphere
LPT	Low-pressure turbine
LE	Leading edge
nac	Nacelle

Abbreviations

BPR	Bypass ratio
CFD	Computational Fluid Dynamics
CST	Commercial Supersonic Technology
FLADE	Fan on Blade
FPR	Fan pressure ratio
GESTPAN	General Stationary and Transient Propulsion Analysis
ICAO	International Civil Aviation Organization
LPT	Low-pressure turbine
MIL-E	Military supersonic inlet standard
MTOM	Maximum take-off mass
OPR	Overall pressure ratio
SFC	Specific fuel consumption
SST	Supersonic transport
STCA	Supersonic Technology Concept Aeroplanes
TIT	Turbine inlet temperature (same as T_4)
UEETP	Ultra-Efficient Engine Technology Program
WEICO	Weight and Cost Estimation tool
S-H	Sears-Haack

Greek Symbols

α, β, γ	Empirical constant (weight model)
η_{engine}	Overall engine efficiency
η_{fan}	Fan adiabatic efficiency
η_{HPC}	High-pressure compressor efficiency
η_{HPT}	High-pressure turbine efficiency
η_{LPT}	Low-pressure turbine efficiency
Λ	Sweep angle
λ_i	Inboard taper ratio
λ_o	Outboard taper ratio
ψ	Cooling flow ratio

goals for supersonic flight emissions margins [16]. To support goal settings they designed a conceptual eight-passenger 55-tonne trijet business jet for cruising at M 1.4. Their assessments of exhaust and noise emissions were performed alongside the evaluation of advanced take-off techniques to manage close to airport noise emissions. These take-off procedures involve optimizing engine rating at take-off and fly-over certification points [18]. In parallel, there have been multiple efforts to shape the airframe to minimize over-land noise pollution, preferably with ground noise below 70 dB for cruise speeds of M=1.6 and above [19,20]. To this end, the NASA X-59 aircraft was developed [21] and key demonstrator efforts have been performed [22].

Jim et al. [20] conducted a multi-objective optimization study on low-boom supersonic transport planforms. The authors used a surrogate-assisted Bayesian optimization framework to minimize sonic boom loudness, drag, and root bending moment (RBM). Their results highlighted the inherent trade-offs in optimizing low-boom configurations, demonstrating that while a 24% reduction in boom loudness and a 25% decrease in RBM were achievable, these came at the expense of a 5% increase in drag. The study did not consider the impact of the engine and its installation on the optimization result. Rodriguez [23] con-

ducted an integrated optimization of the propulsion and airframe of the Aeron supersonic business jet. The study coupled a nonlinear optimizer with Euler CFD simulations to obtain optimal geometries for engine inlet and nozzle while simultaneously considering the flow over the aircraft.

Rallabhandi and Mavris [24] performed SST design analysis with multi-optimization procedures by keeping the aircraft design and the propulsive engine together in their design space. Using an advanced genetic algorithm combined with their optimization analysis, they developed a robust procedure to provide an appropriate design based on aerodynamics and propulsion requirements. From a number of aircraft planforms and propulsion concepts, their paper suggests that a double-delta wing with a Fan on Blade (FLADE) variable-cycle engine and a canard or T-tail configuration is best suited for the mission studied.

Bruckner [25] reported on the conceptual design of a propulsion system for a six-seat SST jet aiming for a range of 4000 nm and a cruise Mach number of 2.0. The final design achieved an 81 percent reduction in landing and take-off NO_x emissions and a 23 percent decrease in fuel burn compared to the baseline technology. The advancements were achieved by inserting technologies developed under the Ultra-Efficient

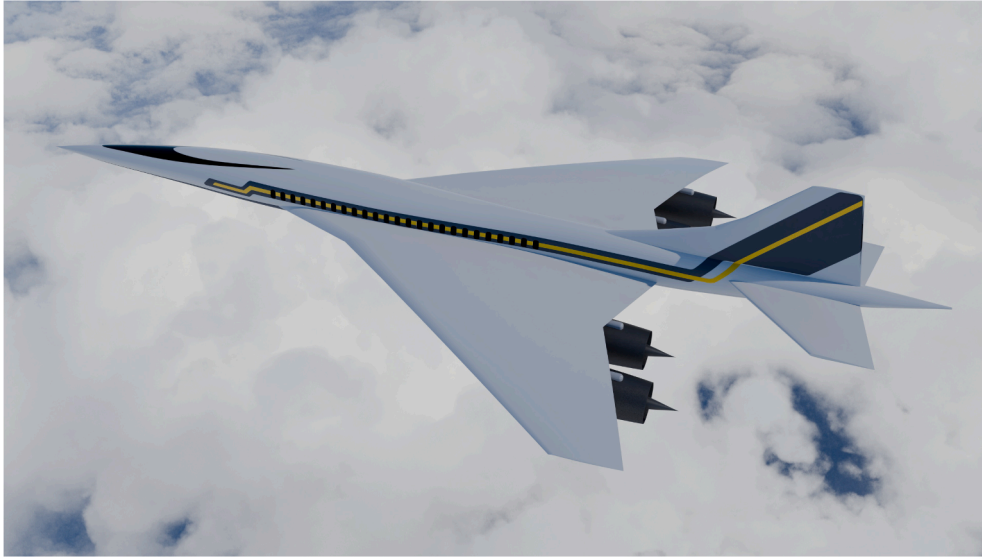


Fig. 1. The SST aircraft concept studied herein.

Engine Technology (UEETP) program and by optimizing the propulsion system for the new component performance.

Brear et al. [26] studied propulsion systems for supersonic aircraft that support the trans-Pacific distance of approximately 6,000 nm aiming for a cruise condition of Mach 2.0 and 60 kft altitude. Their "best case" design achieved a cruise SFC of 26.3 g/kN·s for a turbine inlet temperature of 1940 K. The study did not include installation effects such as the prediction of nacelle drag and engine weight.

Schlette and Staudacher [27] conducted a preliminary engine design study for supersonic business jets, targeting optimal performance for a cruise Mach number of 1.4. This Mach number is lower than the cruise speeds targeted for larger supersonic aircraft such as the one studied in this work. Their research identifies an ideal fan hub-to-tip ratio similar to military fans and discusses compromises between turbine mass and size, highlighting the need for further development in supersonic engine design. The authors claim that a two-stage fan configuration with a specific thrust of approximately 300 m/s enhances the aircraft's range by 11 percent over a single-stage fan. The paper limited the single stage fan pressure ratio (FPR) to a range of 1.6-1.8, which is estimated to give a suboptimal fan design, in particular for the higher Mach number studied in this work. The limit in FPR will increase the diameter of the fan, thereby increasing nacelle drag.

Prashanth et al. [28] conducted a fundamental comparison of the performance, noise, and NO_x emissions constraints of a clean-sheet fully purpose-built turbofan and a derivative supersonic engine (donor core). Their research indicates that while derivative engines meet subsonic NO_x standards with a 6–18 percent margin, clean-sheet engines require adjustments for compliance. For instance, their designed clean-sheet engine showed a 4.5 percent improvement in SFC, but a 2.5 times higher NO_x and 1.2 dB higher noise emissions were encountered. They then discussed trade-offs in engine design, with derivative engines achieving noise levels within 3 EPNdB of clean-sheet engines. By imposing NO_x -level constraints on the clean-sheet engine to be less than for the derivative engine, a 0.5 percent improvement in SFC and 0.8 dB lower noise is achieved. The authors did not consider using a two-stage fan architecture in their study.

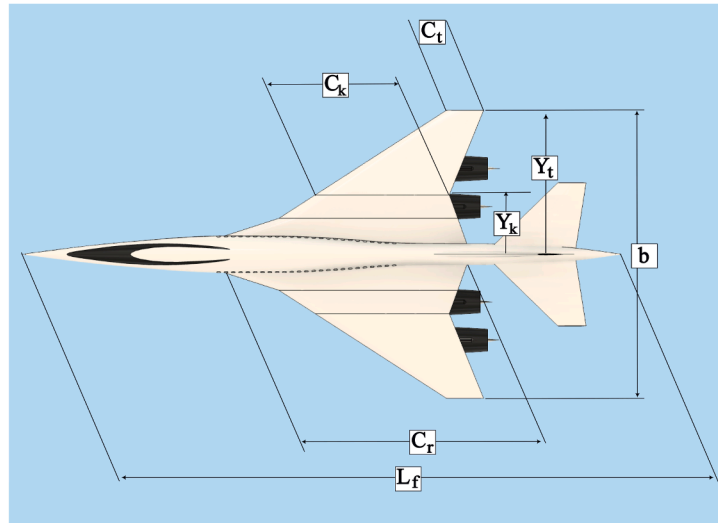
The paper first describes the aircraft concept studied, as illustrated in Figs. 1 and 2, which is representative of a medium-size supersonic transport configuration similar to the Boom Overture aircraft. The paper then goes on to detail the engine design requirements and the submodels for

engine weight modelling, the nacelle drag estimation and the cooling requirement calculations. Subsequently, new results are presented on the aero-thermodynamic performance of the propulsion system, with a comparison between single-stage and two-stage fan architecture. In contrast to earlier studies focused on lower cruise Mach numbers and supersonic business jets, this work targets a cruise Mach number of 1.7 more relevant to larger supersonic aircraft. A parametric study is then presented identifying the optimal operating conditions by varying key propulsion parameters, including FPR, bypass ratio (BPR), and high-pressure turbine inlet temperature. The analysis accounts for the trade-off between engine performance, engine weight, and nacelle drag by coupling separate sub-models and evaluating the specific range of the aircraft. Finally, we evaluate the option of supersonic over-land operation by quantifying the penalty in specific range associated with increasing the Mach number from 0.95 to 1.2.

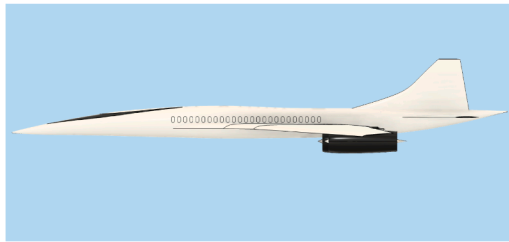
2. SST aircraft concept

As depicted in Fig. 2, the aircraft planform used in this study features a multi-section wing design inspired by NASA's conceptual studies [29]. According to their findings, the double-delta trapezoidal wing configuration offers significantly improved aerodynamic performance for high-altitude supersonic cruise. The cranked wing structure incorporates inboard and outboard leading-edge angles of 73.3° and 52° , respectively. Notably, the updated wing design of the Concorde's ATSF version [30] was based on a similar structural layout as the aircraft planform used in this study.

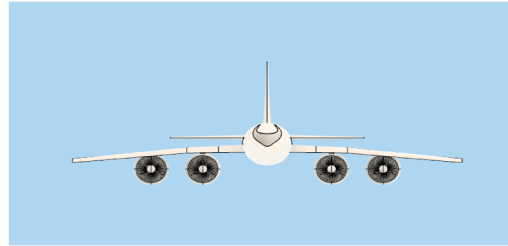
The aircraft length and span in the present study are 65 and 32 m respectively, set to agree with data proposed by the Boom Supersonic Inc. [14]. Their design, the Overture aircraft, is stated to fit approximately 85 passengers and crew members on board. The maximum take-off weight was estimated based on historical data for the Concorde aircraft and its proposed successor the ATSF version [30], resulting in an estimated total mass at take-off (MTOM) of approximately 175,000 kg, and a mid cruise mass of 131,000 kg. The reference area S_r was estimated to provide a sufficient lift based on the cruise speed and the mid cruise mass. The wetted area was estimated from the ATSF wetted to reference area ratio. Sweep angles were estimated based on first principles and the cruise speed proposed [31]. The key airframe parameters are presented in Table 1.



(a) Planform view



(b) Side view



(c) Front view

Fig. 2. Three-view of SST aircraft concept.

Table 1
Aircraft design specifications as defined in Fig. 2.

Parameter	Value	Unit
L_f	65	m
b	32	m
C_r	32	m
C_t	3.2	m
C_k	10.66	m
λ_i	0.33	-
λ_o	0.3	-
AR	3.09	-
Y_k	6	m
Y_t	15	m
S_{ref}	440	m ²
S_w	1365	m ²
M_{mid}	131,000	kg

Table 2
Specific range (SR) as a function of BPR and FPR for two T_4 values.

(a) $T_4 = 1750$ K.		
BPR	FPR	SR
2.5	2.0	112
	2.5	104
	3.0	73
3.0	2.0	110
	2.5	88
	3.0	42
3.5	2.0	102
	2.5	67
	3.0	-
(b) $T_4 = 1850$ K.		
BPR	FPR	SR
2.5	2.0	115
	2.5	113
	3.0	98
3.0	2.0	117
	2.5	111
	3.0	89
3.5	2.0	117
	2.5	102
	3.0	69

3. Propulsion system

The engine performance analysis is performed using the General Stationary and Transient Propulsion ANalysis (GESTPAN) framework, a multidisciplinary tool for gas turbine engine analysis developed at Chalmers University [32]. The conceptual aircraft design tool is coupled with the core engine code enabling the system analysis.

One of the key parameters for evaluating the engine performance is the overall pressure ratio (OPR). For a high speed application like the current SST, the choice of material for the last stages of the compressor sets its temperature capability. This temperature, the maximum allowable compressor exit temperature (T3), in turn determines the possible OPR based on the compressor efficiency. In this work we use a T3 of 970 K, which is very close to the assumption made for the SST appli-

cation presented in [34]. This then translates to an OPR of 33. At take-off the temperature is substantially lower, estimated at around 660 K at hot-day, meaning that it is the cruise condition that limits the OPR. On longer term it is anticipated that the allowable T3 temperatures may continue to rise, ultimately as high as 1070 K [35], but such a high value

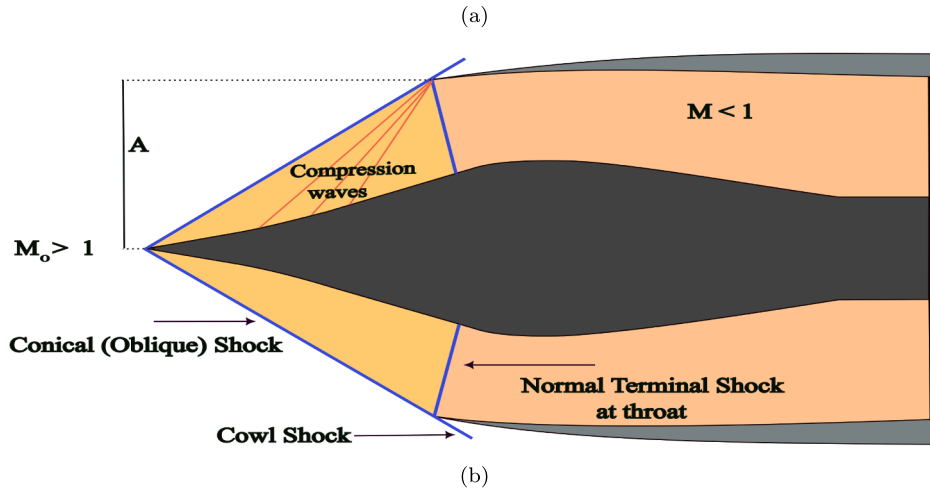
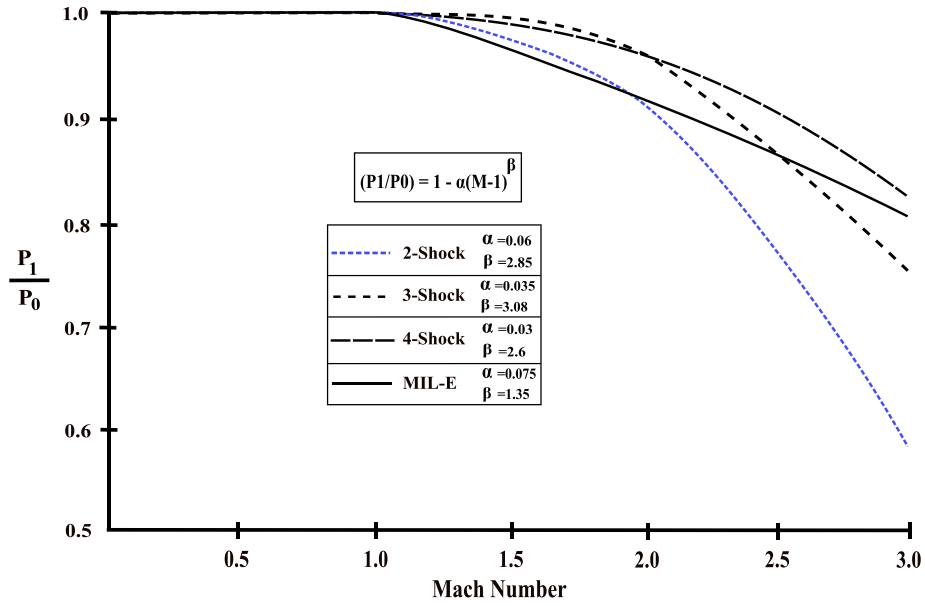


Fig. 3. Supersonic intake pressure recovery diagram (a) [33], and a schematic of an axisymmetric spike inlet (b).

was not viewed feasible for extended periods of running as planned for the SST cruise phase. For T4 we again line-up our assumption with Kharina et al. assuming a maximum of 1850 K [34]. On longer term it may be possible to use higher turbine inlet temperatures, as high as 1950 [35], but again such a high temperature is currently not deemed feasible for longer duration cruise phase operation.

Four 160 kN underwing-mounted turbofan engines power the SST aircraft concept. A two-spool mixed-flow non-afterburning turbofan engine is considered in line with the Symphony engine architecture, as proposed by Boom Supersonic Inc. [14]. An external compression Oswatitsch intake is assumed, also consistent with the Boom aircraft company suggestions, see Figs. 2 and 3. Based on the pressure recovery diagram shown in Fig. 3 and more recent calculations on this type of inlet for a cruise Mach of 1.7 [36], a total pressure loss of 97.8 % was assumed. For fan architecture, two designs are considered for the turbofan in this study; single-stage and two-stage. The stage efficiencies are calculated from:

$$\eta_{stage} = 0.965 - 0.08(\pi_{stage} - 1) \quad (1)$$

using the stage pressure ratio π_{stage} , where the original expression reported in [37] has been updated for a year 2040 entry into service prediction [38].

3.1. Turbine cooling model

For subsonic aircraft, the design of the cooling system is set by the take-off conditions. This is because the highest temperature levels occur in this condition for that type of aircraft. However, supersonic transports designed for a Mach number of 1.7, generate higher working temperatures in cruise than in take-off. For ISA conditions, the increase due to stagnation give an intake stagnation temperature of above 340 K.

Having the OPR fixed at 33, as explained in the previous section, a correlation for estimating the cooling air could then be derived solely dependent on the turbine inlet temperature T_4 . The model underlying the correlation is based on the work by Wilcock et al [39,40]. The cooling flow fraction could be reduced to vary according to:

$$\psi = \frac{\dot{m}_c}{\dot{m}_g} = 0.3140 \left(\frac{T_4}{1500} \right)^2 - 0.1897 \left(\frac{T_4}{1500} \right) - 0.0440 \quad (2)$$

where \dot{m}_g is the mass flow of gas and \dot{m}_c is the mass flow of cooling air. The correlation above agrees closely with the Wilcock's model for a T_4 range between 1750 and 1950 K.

3.2. Propulsion system weight modeling

The propulsion system weight modeling was conducted using WEICO (WEight and COst estimation), an in-house module integrated within the GESTPAN engine performance code. WEICO is based on methods similar to those found in [41] and has been validated and refined through its application in multiple EU projects [42–44]. WEICO provides the propulsion system weight based on correlations that allow the individual engine components to be sized. Then, these sizes are used to estimate component weights that sum up to whole propulsion system weight. Rather than to couple the WEICO tool directly to GESTPAN we have chosen to use WEICO to generate coefficients for a propulsion system weight correlation. This allows us to present the used method explicitly as part of this work. The correlation accounts for the key design parameters being the engine mass flow \dot{m}_a , FPR, BPR, and the high-pressure compressor temperature rise (ΔT_{HPC}). The high-pressure compressor temperature rise is used as a correlation parameter rather than OPR, since the temperature rise relates more directly to work and stage loading than pressure rise. The correlation used for the propulsion system weight is:

$$\text{Mass}_{\text{LP-sys}} = C_1 \cdot \dot{m}_a \cdot (1 + \alpha \cdot (\text{FPR} - 1)) \quad (3)$$

$$\text{Mass}_{\text{Nozzle}} = \dot{m}_a \cdot (C_2 + \beta \cdot (\text{FPR} - 1)) \quad (4)$$

$$\text{Mass}_{\text{HP-sys}} = \dot{m}_a \cdot \frac{C_3 + C_4 \cdot \Delta T_{\text{HPC}}}{(1 + \text{BPR}) \cdot \text{FPR}} \quad (5)$$

where the constants α , β , γ , C_1 , C_2 , C_3 , and C_4 are optimized to align the predicted weights with WEICO outputs. The resulting optimal values are:

$$\alpha = 0.339, \quad \beta = 0.319, \quad \gamma = 0.259 \\ C_1 = 2.48, \quad C_2 = 0.51, \quad C_3 = 5.142, \quad C_4 = 0.01706$$

Comparison between propulsion system weight estimates obtained from WEICO and those computed using the optimized correlation indicate that the maximum deviation between the two methods remains below 9%, demonstrating that the constants yield sufficiently accurate estimates for preliminary design studies.

3.3. Nacelle drag prediction

The nacelle drag calculation in this study follows the supersonic parasite drag method for a revolutionary body in Raymer [33]. The friction and wave drag are the dominant components of drag for nacelle drag prediction. The friction drag coefficient equation is as follows:

$$C_f = \frac{0.455}{(\log_{10} Re)^{2.58} (1 + 0.144 M^2)^{0.65}} \quad (6)$$

where the Re is calculated based on the nacelle dimensions. The nacelle diameter (d_{nac}) is calculated with a factor of 1.1 of the fan diameter (d_{fan}), and the nacelle aspect ratio (AR_{nac}) is set to 4.0, hence, the nacelle length (l_{nac}) is then calculated. It is worth noting that Eq. (6) expresses the turbulent form of the nacelle skin friction drag. On the other hand, the wave drag coefficient for the volume of an axisymmetric body is followed by [45]:

$$C_{D_{\text{wave}}} = 1.1725 \cdot \left(\frac{d_{nac}}{l_{nac}} \right)^2 \cdot \left(\frac{A_{nac}}{S_{\text{ref}}} \right) \quad (7)$$

3.4. Numerical modelling

A general model for a coupled engine and aircraft system results in a semi-explicit ordinary differential algebraic system, i.e.:

$$\mathbf{x}' = f(\mathbf{x}, \mathbf{z})$$

$$\mathbf{0} = g(\mathbf{x}, \mathbf{z}, \boldsymbol{\theta}) \quad (8)$$

where \mathbf{x} constitutes the differential variables and \mathbf{z} represent the algebraic variables. The $\boldsymbol{\theta}$ -vector represent aero-thermodynamic design parameters such as component pressure ratios and flows allowing for parametric studies and multidisciplinary optimization [46–48]. Unless particular transient behavior needs to be resolved such as re-acceleration of the engine in conjunction with a baulked landing or analysis performed for control purposes of the engine, the engine dynamics may be treated as quasi-steady for aircraft mission analysis. If so, only the aircraft performance is treated as transient and the engine is represented by a system of non-linear equations [49]. By being able to model the coupled aircraft engine system as represented by Eq. (8) many of the fundamental non-linearities of the flow and structural couplings [50,51] are not fully resolved but are embedded in the parametric modeling approach.

Convergence is always challenging for a non-linear system of equations and cannot be guaranteed unless good starting estimates are provided. Dynamic modeling is computed using a k th order Backward Differentiation Formula solving for the differential and algebraic variables simultaneously. The algebraic systems are solved using a quasi-Newton method implementing a Broydn update [52] for the Jacobian. Starting estimates are obtained by successively building a full design iteration scheme from subsystems [32] and convergence is set a few order of magnitude larger than the machine precision, that is a normalized sum of squares smaller than 10^{-14} .

4. Results and discussions

The engine performance analysis and design is carried out in accordance with the prescribed airframe specifications and cruise conditions at Mach 1.7. The study provides both single-stage and two-stage intake fan configurations to assess their relative merits. A parametric sweep is conducted over key design parameters, including the FPR, BPR, and high-pressure turbine inlet temperature. The impact of these variations on thrust, specific fuel consumption (SFC), specific range, and overall efficiency is examined to provide insights into optimal design trade-offs.

Following the validation of the computational model, a detailed design-space exploration is performed to compare the aerodynamic and thermodynamic performance during cruise. The subsequent sections will present a quantitative assessment of single-stage and two-stage fan configurations, highlighting their advantages and limitations in the context of supersonic transport propulsion.

4.1. Validation

An option for validation of the aircraft model would be to compare its output with other tools [53] or higher fidelity CFD studies [54]. Here, we validate our aircraft modeling by direct comparison against Concorde data, as reported in [45,55]. The Concorde remains the most well-documented supersonic transport aircraft [56], with datasets for benchmarking engine and aerodynamic performance [57]. The supersonic parasitic drag coefficient (C_{D0}), a critical parameter influencing overall aerodynamic efficiency is depicted in Fig. 4. The comparison with empirical data demonstrates an excellent agreement over a large Mach number range.

Given that the fuselage aerodynamics of a well-designed supersonic transport aircraft approximately follows the Sears-Haack body distribution, an empirical efficiency factor, E_{wd} , may be introduced to account for deviations from the Sears-Haack limit [33]. Typically, for supersonic configurations, E_{wd} ranges between 1.8 and 2.2. The analysis indicates that setting $E_{wd} = 2.0$ yields the best agreement between the computed data and the validation data. This alignment suggests that the adopted aerodynamic modeling captures the essential drag characteristics with reasonable accuracy. The expression for the wave drag [33] is given by Eq. (9). The skin friction coefficient for the fuselage, wings and tail components use Eq. (6) with individual form factors as listed in [33] for the

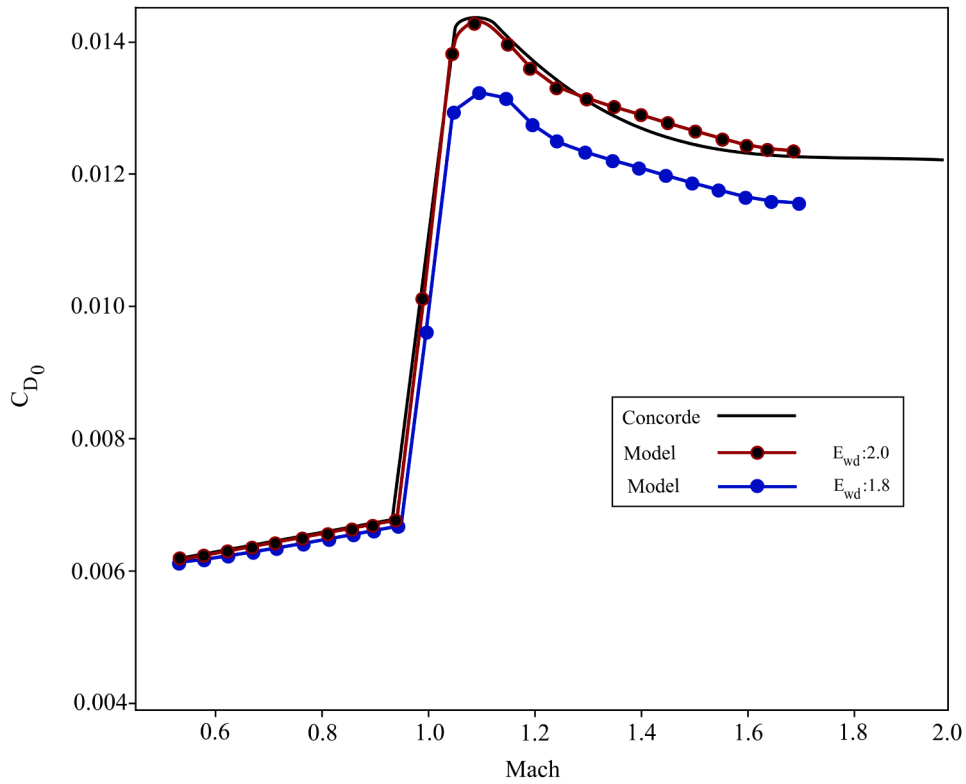


Fig. 4. Comparison of computed zero-lift drag coefficient (C_{D0}) with Concorde reference data [45,55] for validation of the aero-thermodynamic model.

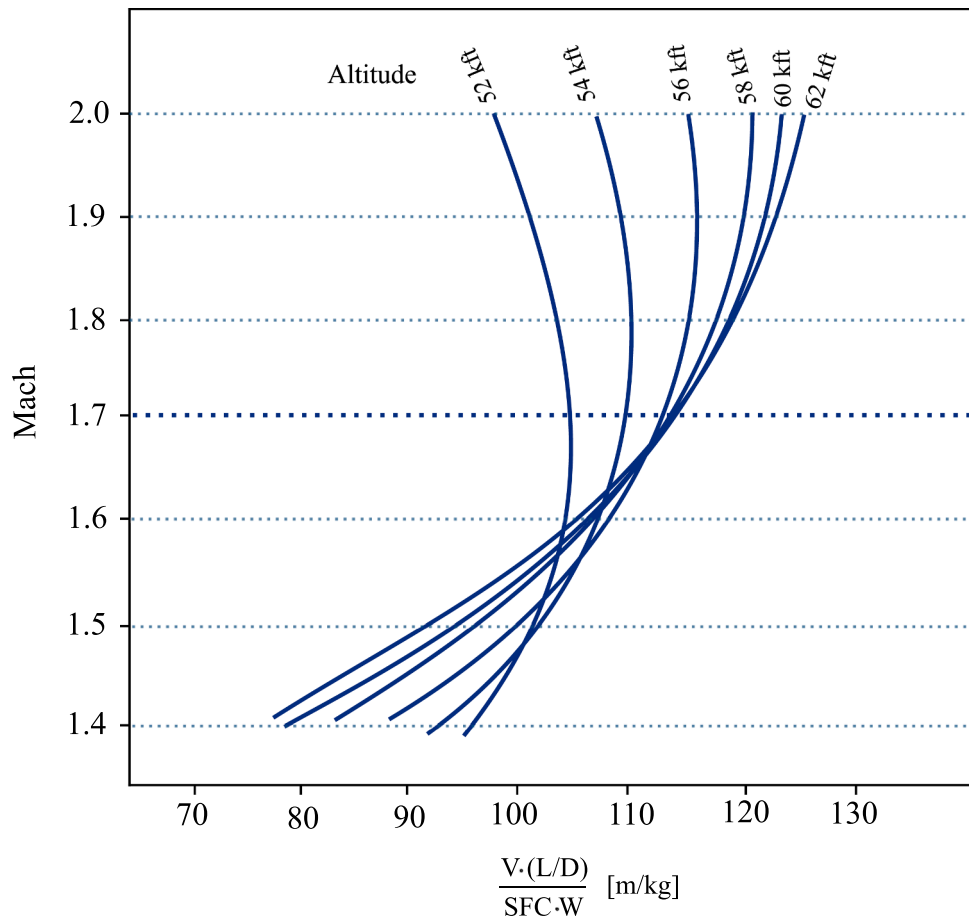


Fig. 5. Cruise specific range at different flight speeds and altitudes.

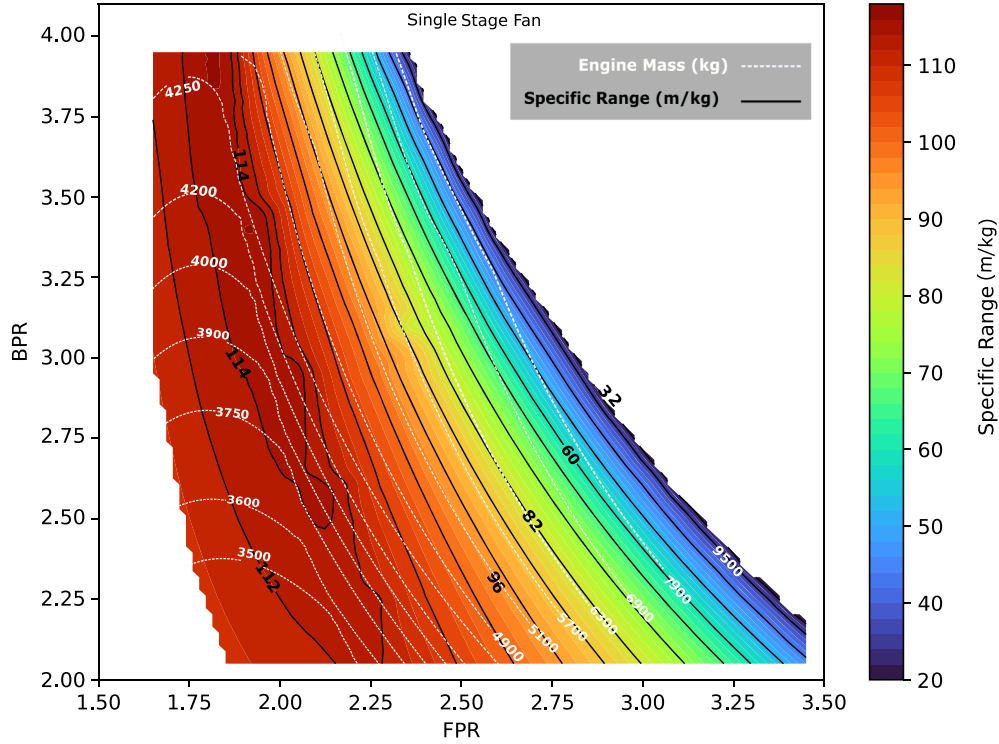


Fig. 6. Feasible design space for the single-stage fan engine configuration for achieving efficient cruise performance at Mach 1.7.

respective components.

$$\left(\frac{D}{q}\right)_{\text{wave}} = E_{WD} \left[1 - 0.386(M - 1.2)^{0.57} \left(1 - \frac{\pi \Lambda_{LE}}{100} \right) \right] \left(\frac{D}{q}\right)_{S-H} \quad (9)$$

The propulsion system validation is split in three parts; engine performance modeling, engine weight modeling and nacelle drag analysis. The methods used for performance modeling have been presented in a previous publication [32], which details the analytic models forming the basis of the propulsion system component calculations. The engine is built up by interconnected components having minimal interfaces, typically sharing a number of single value fluid properties such as pressures, temperatures and mass flows with downstream components [32]. If sufficiently many fluid data are listed in a particular performance point, the engine condition becomes well-defined allowing other researchers to repeat the study. It has been our ambition to list sufficiently many performance parameters in Table 3 to allow repeating our simulation in a commercial [58] or in-house performance tool. Engine weight modelling is derived from an in-house tool validated through a number of EU-projects projects [42–44]. Using the output from the weight modeling tool, we established a reduced order model completely contained within in this paper. This model was then used to compute the weights as part of the multidisciplinary optimization. The nacelle drag modeling was based on previously published material provided by Yoshida et al [45].

4.2. Design analysis

The specific range (SR) is employed as the principal metric for evaluating mission performance, as it directly correlates fuel efficiency with aerodynamic and propulsion characteristics. By analyzing the SR distribution, optimal engine operating conditions can be determined within the defined design space.

To assess the cruise efficiency, a parametric study is performed, examining the interplay between aerodynamic and propulsion characteristics. Fig. 5 illustrates the effect of cruise altitude on mission efficiency,

Table 3

Comparison of key engine performance parameters for optimal single-stage and two-stage fan configurations at design cruise conditions.

Parameter	Unit	Single-stage	Two-stage
Mach	–	1.7	1.7
Altitude	kft	60	60
ΔT_{ISA}	K	0	0
ΔT_{HPC}	K	418.42	389.6
T_3	K	971.40	965.17
T_4	K	1850	1850
BPR	–	3.10	2.85
OPR	–	33	33
Ψ	–	0.203	0.203
Core mass flow	kg/s	49.41	45.93
Fuel flow	kg/s	1.129	1.091
SFC	mg/N-s	25.12	24.64
Fan diameter	m	2.016	1.880
π_{fan}	–	1.88	2.20
η_{fan}	%	89.46	92.63
$\eta_{thermal}$	%	57.9	60.8
η_{engine}	%	46.14	47.12
C_L	–	0.200	0.198
C_D	–	0.027	0.026
L/D	–	7.41	7.45
Engine mass	kg	3851	3548

considering both aerodynamic performance and engine operating characteristics. The figure indicates that for a cruise at Mach 1.7, an altitude in the range of 56,000 to 62,000 feet is feasible. 60,000 and 62,000 offer nearly identical performance and here we choose the 60,000 feet cruise altitude to remain consistent with Concorde and the Overture concept aircraft.

Additionally, key engine parameters, including total engine mass and fan diameter, are depicted in each figure. These parameters are crucial in assessing the trade-offs between aerodynamic efficiency, weight constraints, and propulsion system integration. A well-balanced design

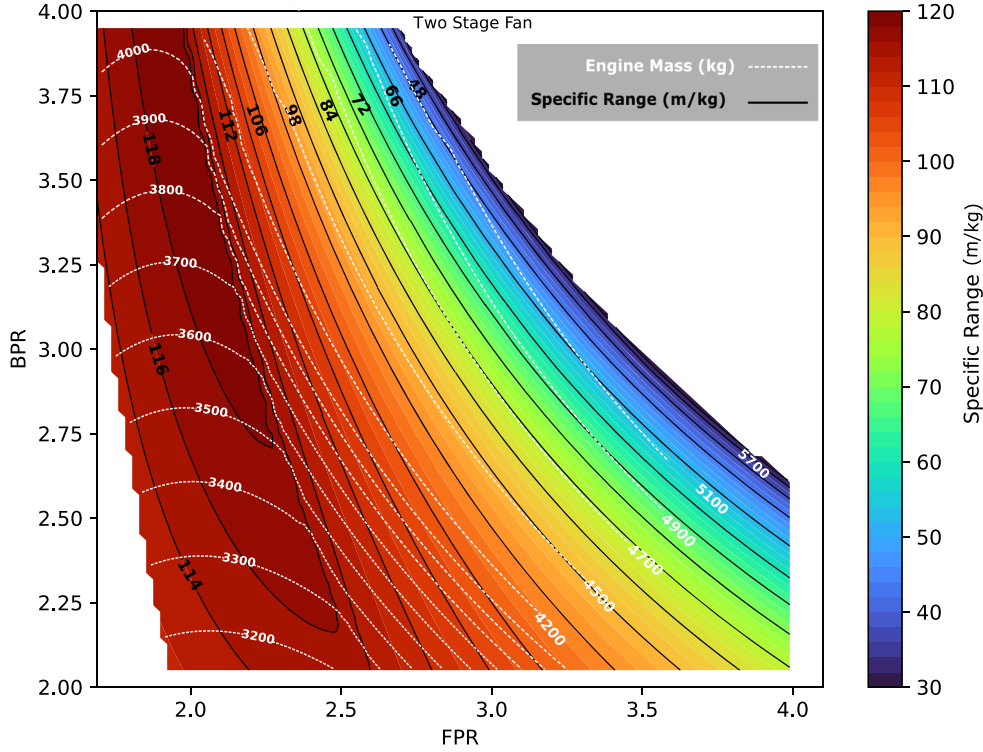


Fig. 7. Feasible design space for the two-stage fan engine configuration for achieving efficient cruise performance at Mach 1.7.

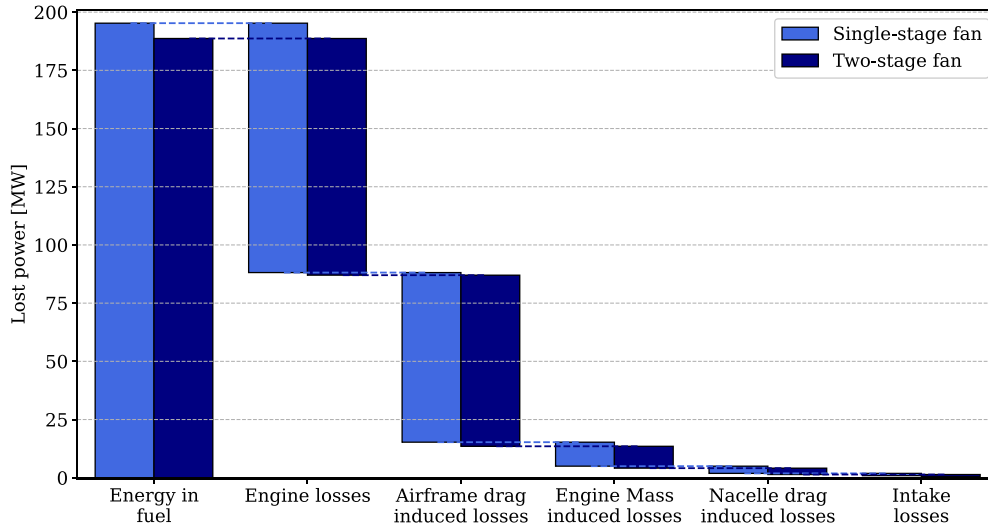


Fig. 8. Lost power computed for aircraft, propulsion system and its installation.

ensures that both thrust and fuel consumption are optimized while maintaining practical weight and dimensional constraints for the supersonic transport aircraft.

The SR is defined as:

$$SR = \frac{V \cdot \frac{L}{D}}{SFC \cdot W} \quad (10)$$

where V is the true airspeed, L/D is the lift-to-drag ratio, SFC represents the specific fuel consumption, and W denotes the aircraft weight. This formulation quantifies the propulsion system efficiency in sustaining flight range per unit of fuel consumed. Maximizing SR is a fundamental objective in supersonic transport optimization, as it dictates the achievable range for a given fuel load. The subsequent analysis delves into the influence of fan stage configuration on SR

and evaluates the optimal design parameters for enhancing mission efficiency.

Having defined a maximum $T3$ and $T4$, as discussed in Section 3, FPR and BPR are now swept within the ranges of 1.6-4.0 and 2.0-4.0, respectively. To achieve high-resolution performance mapping, a step interval of 0.01 is adopted for both FPR and BPR , leading to approximately 10,000 distinct operating conditions being simulated in GESTPAN for each design case (single and two-stage fan configurations). To support the claim that the best specific range is obtained at 1850 K, that is at the maximum allowed turbine inlet temperature, a parametric study was performed for the two-stage architecture also at 1750 K. The key results are collected in Table 2, illustrating that the peak specific range occurs at 1850 K close to the BPR 3.0 triplet.

Table 4
Comparison of performance parameters for single-stage and two-stage fan configurations at design and off-design operating points.

Operating point	Single-stage			Two-stage		
	$M = 0.95$ $h = 27.5$	$M = 1.2$ $h = 40.0$	$M = 1.7$ $h = 60.0$	$M = 0.95$ $h = 27.5$	$M = 1.2$ $h = 40.0$	$M = 1.7$ $h = 60.0$ [kft]
Thrust (kN)	113.5	180.23	179.902	112.57	179.08	177.250
SFC (mg/N·s)	21.27	20.78	24.64	20.62	20.24	25.12
OPR	17.39	28.79	33.0	16.35	26.21	33.0
Fuel Flow (kg/s)	0.6037	0.9365	1.09	0.5808	0.915	1.0129
$C_{f,nac}$	20.14e-4	20e-4	0.0019	20.27e-4	20.13e-4	0.0019
$C_{d,wave,nac}$	13.15e-7	26.32e-5	76.03e-5	7.82e-7	16.29e-5	66.37e-5
C_L	0.1064	0.1218	0.2	0.1081	0.1231	0.198
C_{D0}	0.006212	0.01352	0.0125	0.00625	0.01357	0.0123
L/D	12.05	7.26	7.43	12.08	7.38	7.64
SR (m/kg)	144.4	112.55	114.9	147.42	115.9	119.2

For optimal engine performance, the total pressure ratio between the bypass duct exit ($P_{T5'}$) and the low-pressure turbine exit (P_{T5}) is maintained as close to unity as possible at the mixer entry. This ensures efficient mixing of the core and bypass streams, which is a critical factor in reducing total pressure losses and enhancing overall propulsive efficiency [59]. Maintaining this balance mitigates entropy generation and improves the thermodynamic effectiveness of the propulsion system.

The performance characteristics of the single-stage and two-stage fan engine configurations are evaluated based on the specific range (SR), fan diameter, and total engine mass. Figs. 6 and 7 illustrate the feasible design spaces for these two configurations, highlighting the optimal regions for achieving efficient cruise performance at Mach 1.7.

The specific range, which serves as the primary metric for propulsion efficiency, exhibits a distinct dependency on the FPR and BPR. For the single-stage fan configuration, Fig. 6, the maximum specific range values exceed 114 m/kg and are observed within the FPR range of approximately 1.8-2.1 and a BPR of 2.7-3.2. This region represents the optimal balance between aerodynamic efficiency and fuel consumption. The corresponding fan diameters in this zone range from approximately 1.95 m to 2.15 m, while the engine mass remains within 3650-4000 kg range.

For the two-stage fan configuration, Fig. 7, the design space shifts slightly, with the maximum specific range values surpassing 118 m/kg. The optimal SR region is observed at an FPR of 2.2-2.45 and a BPR of 2.7-3.2. The associated fan diameters range from 1.85 m to 1.95 m, while the engine mass is falling within 3450-3700 kg range which is lower than the single-stage design. The two-stage configuration enables a more refined balance between aerodynamic and thermodynamic efficiencies, allowing for reduced fan diameter while maintaining high performance.

Table 3 presents the key performance parameters for the single-stage and two-stage fan engines at the optimal cruise condition of Mach 1.7 and an altitude of 60,000 feet. The two-stage fan configuration exhibits clear performance benefits over the single-stage design. The SFC is reduced by approximately 1.9%, while the thermal efficiency increases by about 5%. Furthermore, the engine and nacelle masses decrease by nearly 8% and 6.5%, respectively, primarily due to the smaller fan diameter (6.8% reduction), which also lowers the nacelle frontal area and hence the associated wave drag at supersonic cruise. Although the propulsive efficiency shows a marginal decrease of roughly 2%, the combined aerodynamic and thermodynamic effects result in an overall improvement of about 3.5% in the specific range. This indicates that the two-stage fan architecture offers a more balanced and efficient propulsion solution for supersonic transport applications.

4.3. Off-design performance analysis

To better understand over land performance of the SST aircraft concept the single-stage and two-stage fan configurations are evaluated in off-design condition, as detailed in Table 4. The analysis considers flight

at Mach 0.95 and Mach 1.2 at operational altitudes of 27.5 kft and 40 kft, respectively. The altitudes used for each flight speed were selected by finding the maximum specific range in the same way as already discussed for the selection of the cruise altitude, see Fig. 5. The Mach 0.95 condition corresponds to start of transonic drag rise, see Fig. 4, whereas the Mach 1.2 point is in the Mach 1.1-1.3 supersonic regime for which overland boom-less flight has been discussed for the Overture aircraft.

Overland boom-less cruise has been brought forward as a means to increase future SST airline profitability. Table 4 reveals that there is a substantial penalty for operating in the suggested boom-less overland Mach range, here represented by the Mach 1.2 condition. We compute a specific range penalty of 22% going from transonic Mach 0.95 flight to supersonic overland cruise. The penalty arises from the rapid drop in lift-to-drag which is only partially counteracted by the increased Mach number combined with a relatively modest decrease in SFC.

4.4. Overall loss breakdown

To understand the key drivers for inefficiency we present a loss breakdown for the aircraft computed to the same currency, namely lost work as illustrated in Fig. 8. From the close to 190 MW of power contained in the fuel used for the two stage fan configuration, around 54% or 102 MW of the losses are associated with the engine. Airframe drag induced losses represent close to 39% or 73.5 MW of losses. Installation related losses are broken down into additional drag needed to carry the engine mass (lift induced losses) being 5.0%, nacelle drag losses of 1.45% and intake losses of 0.5%.

5. Conclusion

An aero-thermodynamic assessment has been performed to compare the single-stage and two-stage fan architectures for a supersonic transport propulsion system operating at Mach 1.7 and 60,000 ft. The design-space exploration revealed that the two-stage fan yields superior cruise performance, achieving a specific range of 118 m/kg compared to 114 m/kg for the single-stage configuration. At the optimal design point, the two-stage fan attains a 1.9% reduction in specific fuel consumption and a 5% improvement in thermal efficiency, while simultaneously lowering the fan diameter by 6.7% and the total engine masses by approximately 7.9%. These combined effects enhance overall propulsive and aerodynamic efficiency, providing a more optimal configuration suitable for sustained supersonic cruise. The best cruise performance, calculated for the two-stage configuration, was obtained at a BPR of 2.85 and an FPR of 2.2. The T_4 1850 K case produced a higher specific range than the 1750 K case, despite a 23% increase in coolant flow need.

The off-design analysis reveals a significant performance penalty associated with the long-proposed idea of boom-less, overland supersonic cruise. Our estimate calculates a 22% reduction in specific range when shifting from transonic Mach 0.95 to supersonic overland cruise. This

drop is driven primarily by a sharp decrease in lift-to-drag ratio, only partly offset by the higher cruise Mach number and a modest improvement in SFC.

CRedit authorship contribution statement

Mehdi Habibniam: Writing – original draft, Visualization, Validation, Software, Methodology, Investigation, Data curation, Conceptualization; **Anders Lundblad:** Writing – review & editing, Supervision, Project administration, Funding acquisition; **Arthur Rizzi:** Writing – review & editing; **Jesper Ooppelstrup:** Writing – review & editing; **Tomas Grönstedt:** Writing – review & editing.

Data availability

Data will be made available on request.

Declaration of competing interest

We confirm that this manuscript has not been published previously and is not under consideration elsewhere. All authors have approved the manuscript and declare no conflicts of interest.

Acknowledgement

This research was funded by the Swedish Governmental Agency for Innovation Systems (VINNOVA), reference number 2023-01543. A special thanks to the students who brought great effort and enthusiasm to the SST design projects supporting the development of this publication, namely Joel Andersson, Aron Olofsson, Axel Lindmark, Andreas Eriksson, Nils Bensryd, Sofia Björs, Tobias Behrendtz, Filip Wilhelmsson, Katarina Arvidsson, Emelie Gillerstedt, Joel Svensjö, Martin Stjernkvist, Lowe Elstig, Paula Eriksson, Viggo Gripestam, Alva Härelind Ingelsten, Adam Persson, Alexander Saal, Alexander Bengtsson, Albin Bertebo, Albin Eriksson, Carl Holmberg, David Holmén, Edward Nijm, Bilal Sid-diqui, Adam Kasicka.

References

- [1] R.L. Bisplinghoff, The supersonic transport, *Sci. Am.* 210 (6) (1964) 25–35.
- [2] F.E. McLean, *Supersonic Cruise Technology*, 472, NASA Scientific and Technical Information Branch, National Aeronautics, 1985.
- [3] J.A. Sabatella, *Advanced Supersonic Propulsion study*, Technical Report, 1974.
- [4] F. Burcham, Jr, R. Ray, T. Conners, K. Walsh, *Propulsion flight research at NASA Dryden from 1967 to 1997*, in: 34th AIAA/ASME/SAE/ASEE Joint Propulsion Conference and Exhibit, 1998, p. 3712.
- [5] W.K.H. Kressner, The 2707 supersonic transport, *Proc. IEEE* 56 (4) (1968) 682–691.
- [6] R.V. Harris, Jr, On the threshold-the outlook for supersonic and hypersonic aircraft, *J. Aircr.* 29 (1) (1992) 10–19. <https://doi.org/10.2514/3.46119>
- [7] British Airways PLC, Concorde Announcement: “End of an Era” (Retirement of the Concorde Fleet), 2003. <https://www.investigate.co.uk/announcement/rms/bay-capital-bay/concorde-announcement-/459026>.
- [8] S. Langmaak, J. Scanlan, A. Söbester, Robust gas turbine and airframe system design in light of uncertain fuel and CO₂ prices, *J. Aircr.* 53 (5) (2016) 1372–1390.
- [9] Z. Chen, Q. Li, et al., From concorde’s atrocious fuel economy and demise of rear-mounted engines to future supersonic transportation, in: AIAA Aviation Forum, 2022. <https://doi.org/10.2514/6.2022-3314>
- [10] P.A. Henne, Case for small supersonic civil aircraft, *J. Aircr.* 42 (3) (2005) 765–774. <https://doi.org/10.2514/1.51119>
- [11] B. Liebhart, K. Lütjens, An analysis of the market environment for supersonic business jets, DLRK Tagungsband 2011: 60. Deutscher Luft-und Raumfahrtkongress in Bremen (2011).
- [12] J. Wen, C.J. Weit, M. Mayakonda, A. Anand, T. Zaidi, D. Mavris, A methodology for supersonic commercial market estimation and environmental impact evaluation (part II), in: AIAA Aviation 2020 Forum, 2020, p. 3261.
- [13] Y. Sun, H. Smith, Review and prospect of supersonic business jet design, *Prog. Aerosp. Sci.* 90 (2017) 12–38. <https://doi.org/10.1016/j.paerosci.2016.12.003>
- [14] Boom Technology Inc., *Overture: Supersonic Airliner*, 2025, (<https://boomsupersonic.com/overture>). Accessed: 2025-12-23.
- [15] Boom Technology Inc., *XB-1 Flight Test Program Live Blog*, 2025, (<https://boomsupersonic.com/flyby/xb-1-live-blog-flight-test-program>). Accessed: 2026-02-21.
- [16] J.J. Berton, D.L. Huff, K. Geiselhart, J. Seidel, Supersonic technology concept aeroplanes for environmental studies, in: AIAA Scitech 2020 Forum, 2020, p. 0263. <https://doi.org/10.2514/6.2020-0263>
- [17] H. Welge, C. Nelson, J. Bonet, Supersonic vehicle systems for the 2020 to 2035 timeframe, in: 28th AIAA Applied Aerodynamics Conference, 2010, p. 4930. <https://doi.org/10.2514/6.2010-4930>
- [18] L.J.A. Voet, P. Prashanth, R.L. Speth, J.S. Sabnis, C.S. Tan, S.R.H. Barrett, Automatic continuous thrust control for supersonic transport takeoff noise reduction, *J. Aircr.* 61 (1) (2024) 291–306. <https://doi.org/10.2514/1.C037394>
- [19] W. Li, K. Geiselhart, Multidisciplinary design optimization of low-boom supersonic aircraft with mission constraints, *AIAA J.* 59 (1) (2021) 165–179. <https://doi.org/10.2514/1.J059237>
- [20] T.M.S. Jim, G.A. Faza, P.S. Palar, K. Shimoyama, A multiobjective surrogate-assisted optimisation and exploration of low-boom supersonic transport platforms, *Aerosp. Sci. Technol.* 128 (2022) 107747.
- [21] J. Rathsam, P. Coen, A. Loubeau, L. Ozoroski, G. Shah, Scope and goals of NASA’s quesst community test campaign with the X-59 aircraft, in: 14th ICBCEN Congress on Noise as a Public Health Problem, 2023.
- [22] A.B. Vaughn, W.J. Doebler, A.W. Christian, Cumulative noise metric design considerations for the NASA quesst community test campaign with the X-59 aircraft, in: INTER-NOISE and NOISE-CON Congress and Conference Proceedings, 268, Institute of Noise Control Engineering, 2023, pp. 1485–1496.
- [23] D. Rodriguez, Propulsion/Airframe integration and optimization on a supersonic business jet, in: 45th AIAA Aerospace Sciences Meeting and Exhibit, 2007, p. 1048.
- [24] S.K. Rallabhandi, D.N. Mavris, Simultaneous airframe and propulsion cycle optimization for supersonic aircraft design, *J. Aircr.* 45 (1) (2008) 38–55. <https://doi.org/10.2514/1.33183>
- [25] R. Bruckner, Conceptual design of a supersonic business jet propulsion system, in: 38th AIAA/ASME/SAE/ASEE Joint Propulsion Conference & Exhibit, 2002, p. 3919. <https://doi.org/10.2514/6.2002-3919>
- [26] M.J. Brear, J.L. Kerrebrock, A.H. Epstein, Propulsion system requirements for long range, supersonic aircraft, *J. Fluids Eng.* (2006). <https://doi.org/10.1115/1.2169810>
- [27] T. Schlette, S. Staudacher, Preliminary design and analysis of supersonic business jet engines, *Aerospace* 9 (9) (2022) 493. <https://doi.org/10.3390/aerospace9090493>
- [28] P. Prashanth, L.J.A. Voet, R.L. Speth, J.S. Sabnis, C.S. Tan, S.R.H. Barrett, Impact of design constraints on noise and emissions of derivative supersonic engines, *J. Propul. Power* 39 (3) (2023) 454–463. <https://doi.org/10.2514/1.B38918>
- [29] H. Jiménez, D.N. Mavris, Conceptual design of current technology and advanced concepts for an efficient multi-mach aircraft, *SAE Trans.* 114 (2005) 1343–1353. <https://doi.org/10.4271/2005-01-3399>
- [30] D. Collard, Future Supersonic Transport Studies at Aerospatiale, Technical Report, SAE Technical Paper, 1990. <https://doi.org/10.4271/901890>
- [31] J.D. Anderson, *Modern Compressible Flow: With Historical Perspective*, 2nd ed., McGraw-Hill, 1990.
- [32] T. Grönstedt, Development of Methods for Analysis and Optimization of Complex Jet Engine Systems, Chalmers Tekniska Hogskola (Sweden), 2000.
- [33] D.P. Raymer, *Aircraft Design: A Conceptual Approach*, American Institute of Aeronautics and Astronautics, Reston, VA, USA, 6th edition, Reston, VA, USA, 2018.
- [34] A. Kharina, D. MacDonald, D. Rutherford, Environmental Performance of Emerging Supersonic Transport Aircraft, Working Paper 2018-06, The International Council on Clean Transportation (ICCT), 2018.
- [35] A. Rolt, V. Sethi, F. Jacob, J. Sebastianpillai, C. Xisto, T. Grönstedt, L. Raffaelli, Scale effects on conventional and intercooled turbofan engine performance, *Aeronaut. J.* 121 (1242) (2017) 1162–1185.
- [36] J.W. Slater, Supersonic external-compression inlets for mach 1.4 to 2.0, in: AIAA Aviation 2023 Forum, 2023, p. 4016.
- [37] A. Sgueglia, P. Schmollgruber, N. Bartoli, O. Atinault, E. Benard, J. Morlier, Exploration and sizing of a large passenger aircraft with distributed ducted electric fans, in: 2018 AIAA Aerospace Sciences Meeting, 2018, p. 1745.
- [38] S. Samuelsson, K.G. Kyrianiadis, T. Grönstedt, Consistent conceptual design and performance modeling of aero engines, in: Turbo Expo: Power for Land, Sea, and Air, 56673, American Society of Mechanical Engineers, 2015, p. V003T06A017.
- [39] R.C. Wilcock, J.B. Young, J.H. Horlock, The effect of turbine blade cooling on the cycle efficiency of gas turbine power cycles, *J. Eng. Gas Turbines Power* 127 (1) (2005) 109–120.
- [40] J.B. Young, R.C. Wilcock, Modeling the air-cooled gas turbine: Part 2-coolant flows and losses, *J. Turbomach.* 124 (2) (2002) 214–221.
- [41] M.T. Tong, I. Halliwell, L.J. Ghosn, A computer code for gas turbine engine weight and disk life estimation, in: Turbo Expo: Power for Land, Sea, and Air, 36061, 2002, pp. 111–118.
- [42] J.-J. Korsia, G. De Spiegeleer, VITAL–European R&D programme for greener aero-Engines, 18th ISABE (2007).
- [43] G. Wilfert, J. Sieber, A. Rolt, N. Baker, A. Touyeras, S. Colantuoni, New environmental friendly aero engine core concepts, ISABE Paper 1120 (2007) 6.
- [44] R. von der Bank, S. Donnerhack, A. Rae, M. Cazalens, A. Lundblad, M. Dietz, Lemcote: improving the core-engine thermal efficiency, in: Turbo Expo: Power for Land, Sea, and Air, 45578, American Society of Mechanical Engineers, 2014, p. V01AT01A001.
- [45] K. Yoshida, Supersonic drag reduction technology in the scaled supersonic experimental airplane project by JAXA, *Prog. Aerosp. Sci.* 45 (4–5) (2009) 124–146.
- [46] J.-x. Leng, Z. Xie, W. Huang, Y. Shen, Z.-g. Wang, Multidisciplinary design optimization of the first-stage waverider based on boost-glide flight trajectory, *Aerosp. Sci. Technol.* 160 (2025) 110033.
- [47] Y. Shen, W. Huang, T.-t. Zhang, L. Yan, Parametric modeling and aerodynamic optimization of EXPERT configuration at hypersonic speeds, *Aerosp. Sci. Technol.* 84 (2019) 641–649.

- [48] Y. Shen, W. Huang, L. Yan, T.-t. Zhang, Constraint-based parameterization using FFD and multi-objective design optimization of a hypersonic vehicle, *Aerosp. Sci. Technol.* 100 (2020) 105788.
- [49] K.E. Brenan, S.L. Campbell, L.R. Petzold, *Numerical Solution of Initial-Value Problems in Differential-Algebraic Equations*, Elsevier Science Publishing Co., Inc., 1989.
- [50] X.-Y. Gao, In plasma physics and fluid dynamics: symbolic computation on a $(2 + 1)$ -dimensional variable-coefficient Sawada-Kotera system, *Appl. Math. Lett.* 159 (2025) 109262.
- [51] C.-H. Feng, B. Tian, X.-T. Gao, Bilinear Bäcklund transformations, as well as n-soliton, breather, fission/fusion and hybrid solutions for a $(3 + 1)$ -dimensional integrable wave equation in a fluid, *Qualit. Theory Dyn. Syst.* 24 (2) (2025) 1–19.
- [52] C.G. Broyden, A New Method of Solving Nonlinear Simultaneous Equations, *The Computer Journal* 12 (1969) 94–99.
- [53] T. Zhang, Z. Wang, W. Huang, D. Ingham, L. Ma, M. Porkashanian, An analysis tool of the rocket-based combined cycle engine and its application in the two-stage-to-orbit mission, *Energy* 193 (2020) 116709.
- [54] M. Ou, L. Yan, W. Huang, T.-t. Zhang, Design exploration of combinational spike and opposing jet concept in hypersonic flows based on CFD calculation and surrogate model, *Acta Astronaut.* 155 (2019) 287–301.
- [55] G. Corning, *Supersonic and Subsonic, CTOL and VTOL, Airplane Design*, 4th edition, College Park, Maryland, 1976.
- [56] A. Rizzi, J. Ooppelstrup, *Aircraft Aerodynamic Design with Computational Software*, Cambridge University Press, 2021.
- [57] C. Leyman, *Case Study by Aerospaciale and British Aerospace on the Concorde*, American Institute of Aeronautics and Astronautics, 1980.
- [58] D.J. Kurzke, G. GmbH, *GasTurb Gas Turbine Performance Simulation Software*, GasTurb GmbH, Aachen, Germany, 2023. Version 15. Comprehensive user manual and software documentation, <https://gasturb.com/>
- [59] P.T. Millhouse, S.C. Kramer, P.I. King, E.F. Mykytka, Identifying optimal fan compressor pressure ratios for the mixed-stream turbofan engine, *J. Propul. Power* 16 (1) (2000) 79–86.